



3D-printed EVA-based patches manufactured by direct powder extrusion for personalized transdermal therapies

Giorgia Maurizii^a, Sofia Moroni^a, Shiva Khorshid^a, Annalisa Aluigi^a, Mattia Tiboni^{a,*}, Luca Casettari^{a,b}

^a Department of Biomolecular Sciences, University of Urbino Carlo Bo, Piazza del Rinascimento, 6, 61029 Urbino, PU, Italy

^b Prospika Srl, Via del Trabocchetto, 1, 61034, Fossombrone, PU, Italy

ARTICLE INFO

Keywords:

Direct Powder Extrusion (DPE)
Ethyl vinyl acetate (EVA) copolymer
Transdermal patches
Personalized medicine

ABSTRACT

In recent years, 3D printing has attracted great interest in the pharmaceutical field as a promising tool for the on-demand manufacturing of patient-centered pharmaceutical forms. Among the existing 3D printing techniques, direct powder extrusion (DPE) resulted as the most practical approach thanks to the possibility to directly process excipients and drugs in a single step. The main goal of this work was to determine whether different grades of ethylene vinyl acetate (EVA) copolymer might be employed as new feedstock materials for the DPE technique to manufacture transdermal patches. By selecting two model drugs with different thermal behavior, (*i.e.*, ibuprofen and diclofenac sodium) we also wanted to pay attention to the versatility of EVA excipient in preparing patches for customized transdermal therapies. EVA was combined with 30 % (w/w) of each model drugs. The physicochemical composition of the printed devices was investigated through Fourier-transform infrared spectroscopy, differential scanning calorimetry, and thermogravimetric analyses. FT-IR spectra confirmed that the starting materials were effectively incorporated into the final formulation, and thermal analyses demonstrated that the extrusion process altered the crystalline morphology of the raw polymers inducing the formation of crystals at lower thicknesses. Lastly, the drug release and permeation profile of the printed systems was evaluated for 48 h and showed to be dependent on the VA content of the EVA grade (74.5 % of ibuprofen released from EVA 4030AC matrix and 12.6 % of diclofenac sodium released from EVA1821A matrix). Hence, this study demonstrated that EVA and direct powder extrusion technique could be promising tools for manufacturing transdermal patches. By selecting the EVA grade with the appropriate VA content, drugs with dissimilar melting points could be printed preserving their thermal stability. Moreover, the desired drug release and permeation profile of the drug can be achieved, representing an important advantage in terms of personalized medicine.

1. Introduction

Over the years, in the pharmaceutical field, the concept of a ‘one-size-fits-all drug’ has been revised to make room for personalized medicine, thanks primarily to the spreading of three-dimensional printing (3DP) (Vaz and Kumar, 2021). This technology allows the manufacturing of pharmaceutical forms with customized shapes, dosages, release characteristics, and drug combinations. The desired object is produced in a layer-by-layer manner by translating a computer-aided design (CAD) model into a solid prototype (Seoane-Viaño et al., 2021; Reddy et al., 2020). Between the advantages conferred, in addition to increasing patient compliance and adherence to treatment, this approach reduces fabrication costs and enables the on-site production of

medicines, potentially performed in hospitals and pharmacies (Fanous et al, 2020).

Among the existing 3D printing techniques, extrusion-based 3D printing methods, such as Fused Deposition Modeling (FDM) and Direct Powder Extrusion (DPE), are the most used for the on-demand manufacturing of pharmaceuticals, thanks to the low cost, flexibility, and the wide availability of materials and printers (Annaji et al., 2020). FDM is based on the extrusion of a drug-loaded thermoplastic filament, conventionally produced by Hot Melt Extrusion (HME). Despite the successful employment of this technique, the two-step thermal processing can cause material degradation, and the need for a filament with optimal rheological and mechanical properties can limit its use (Xu et al., 2020; Goyanes et al., 2019; Boniatti et al., 2021). DPE is an

* Corresponding author.

E-mail address: mattia.tiboni@uniurb.it (M. Tiboni).

<https://doi.org/10.1016/j.ijpharm.2023.122720>

Received 16 December 2022; Received in revised form 8 February 2023; Accepted 9 February 2023

Available online 11 February 2023

0378-5173/© 2023 The Authors. Published by Elsevier B.V. This is an open access article under the CC BY license (<http://creativecommons.org/licenses/by/4.0/>).

alternative to FDM as it permits the direct printing of powder blends and pellets by extrusion through a nozzle, using a single-screw extruder mounted in the printer. By avoiding filament preparation with HME, this single-step production process reduces the thermal stress of active compounds and is more cost-and-time-effective and practical in terms of on-site manufacturing (Ong et al., 2020). Moreover, it potentially allows freedom in formulation selection since the material flow toward the printer nozzle is mostly driven by the screw rotation, and it is slightly influenced by the material's mechanical properties (Borandeh et al., 2021; Sánchez-Guirales et al., 2021; Pistone et al., 2022; Pistone et al., 2023).

Ethylene-vinyl acetate (EVA) is a thermoplastic copolymer of ethylene and vinyl acetate (VA), where the VA units, ranging from 0 % to 40 %, are distributed across the ethylene polymer backbone, affecting its mechanical and physical properties. A higher VA content decreases the polymer's melting point, stiffness, and crystallinity and increases its polarity, flexibility, and adhesion, resulting in a wide spectrum of applications. In the pharmaceutical field, the usage of EVA polymers covers different applications including transdermal drug delivery, intrauterine devices, and subcutaneous implants (Celanese, 2015a). EVA-based formulations were broadly studied as interesting candidates for 3D printing applications thanks to the advantageous features of this material, such as the versatility, the easy extrudability without the addition of any plasticizer, and the low glass transition (Samaro et al., 2021; Schneider et al., 2017). Nevertheless, their compatibility with the DPE technique was poorly tested.

This study aimed to manufacture, for the first time, 3D-printed EVA-based transdermal patches with the DPE technique, given the consolidated utilization of this material in transdermal drug delivery systems (TDDS) as a rate-controlling membrane (Celanese, 2015a). Moreover, the versatility of EVA in preparing patches for personalized transdermal therapies was highlighted by selecting two model drugs with different melting points. Specifically, EVA 1821A (18 % VA), a high melting temperature polymer grade, and EVA 4030AC (40 % VA), a low melting temperature polymer grade, were selected to meet the characteristics of diclofenac sodium and ibuprofen. This is to demonstrate that by selecting the appropriate EVA grade both thermosensitive drugs and drugs requiring high extrusion temperatures can be processed with the DPE technique, obtaining suitable mechanical and physicochemical properties and good morphological quality of the resulting patches. The obtained printed products were physicochemically characterized using Fourier-transform infrared spectroscopy (FTIR), differential scanning calorimetry (DSC), and thermogravimetric analysis (TGA), to study the effect of EVA grade on the characteristics of the drug-loaded patches. Furthermore, their mechanical properties were evaluated with a texture analyzer (TA). Finally, the release and permeation profiles of the model drugs were determined with vertical diffusion cells mounting skin-mimicking membranes.

2. Materials and methods

2.1. Materials

Both grades of ethylene vinyl acetate (EVA) copolymer (Ateva 4030AC and Ateva 1821A), in micronized form, were kindly donated by Celanese (Sulzbach, Germany). Ibuprofen and diclofenac sodium were provided from BASF (Ludwigshafen am Rhein, Germany) and Farmalabor (Canosa di Puglia (BT), Italy) respectively. Strat-M® membranes were purchased from Merck (Milan, Italy). All the solvents used were analytical grade.

2.2. Methods

2.2.1. Direct powder extrusion printing of drug-loaded transdermal patches

Mixtures of EVA 4030AC and ibuprofen (F1), and EVA 1821A and diclofenac sodium (F2) were used as feedstocks for subsequent 3D

Table 1

Composition of the formulations.

Formulation	Ibuprofen (%)	Diclofenac Sodium (%)	EVA 4030AC (%)	EVA 1821A (%)
F1	30	–	70	–
F2	–	30	–	70

printing with direct powder extrusion (Table 1). Each formulation was prepared by carefully weighing the model drug and the polymer, mixing them manually with a mortar and pestle, and then automatically using a powder blender (Galena Top, Ataena Srl, Italy). The defined ibuprofen and diclofenac sodium proportion was 30 % wt to load approximately 1 g of active compound into the 3D printed patch. The prepared blends (approximately 3.5 g each) were then directly added to the hopper of the DPE 3D printer (3D Cultures, USA), which was equipped with a single screw extruder with a nozzle diameter of 1 mm. Key parameters were optimized, including print speed, layer height, and printing temperature. The print speed was set at 10 mm/s and the layer height was 0.6 mm with 100 % of infill density. These print settings remained constant for both formulations. On the contrary, the printing temperature was set according to the drug contained in the formulation and the coupled polymer characteristics. Specifically, after performing DSC analyses, the starting printing temperature of the polymer-drug mixtures was set at approximately 20 °C above the melting temperature of the analyzed pure polymer powder (Table 4), to aid the extrusion process by lowering the flow viscosity of the blends. Consequently, the starting printing temperature of F1 was set at 70 °C and the one of F2 at 110 °C. Several trials were done by gradually increasing the printing temperature until the extruded products' good quality was reached. The optimized temperature for 3D printing of F1 was 80 °C while the one of F2 was 180 °C. Finally, the build plate was kept at 45 °C and covered with an adhesion sheet (Polypropylene, Ultimaker, The Netherlands) to increase adhesion to the plate. The patch geometry (side × height: 70x50 mm) was designed using computer-aided design (CAD) software (Tinkercad®, Autodesk, USA) to create an STL file format compatible with the Ultimaker Cura 4.1 Software (Ultimaker, The Netherlands).

2.2.2. Characterization of 3D printed transdermal patches

2.2.2.1. Morphology, and thickness and weight uniformity. After the printing, the resulting patches were weighed, and their thicknesses were measured to evaluate the reproducibility of the printing process. Thickness measurements were performed using a digital caliper (Mitutoyo, Japan). Average thickness, weight, and standard deviation values were calculated from triplicate measurements. In addition, a digital microscope (Pancellent, China) and an environmental scanning electron microscope (ESEM) (FEI, Hillsboro, OR, USA) were used to investigate the surface morphology of the printed products. For ESEM analysis, the instrument was utilized in low-vacuum mode, with a specimen chamber pressure set from 0.6 to 0.80 mbar, an accelerating voltage of 25 kV, a working distance of 9.6 mm, and a magnification ranging between 700 and 2000×. The samples were gold-sputtered for 1 min before the analysis. The images were obtained by means of a back-scattered electron detector.

2.2.2.2. Content uniformity. Six portions were cut from different sections of the printed patches, weighed, and placed in ethanol to assess the homogeneous distribution and the effective amount of ibuprofen and diclofenac sodium present in each patch. All the samples were shaken continuously for 24 h at 100 rpm. Then, the amount of the drug was measured with high-performance liquid chromatography (HPLC, Agilent 1260 Infinity II, Agilent, USA). For HPLC analysis, the mobile phase consisted of a mixture of 0.5 % formic acid in water and acetonitrile (ratio 20:80) for ibuprofen, and a mixture of 0.5 % formic acid in water and methanol (ratio 30:70) for diclofenac sodium. The flow rate of the

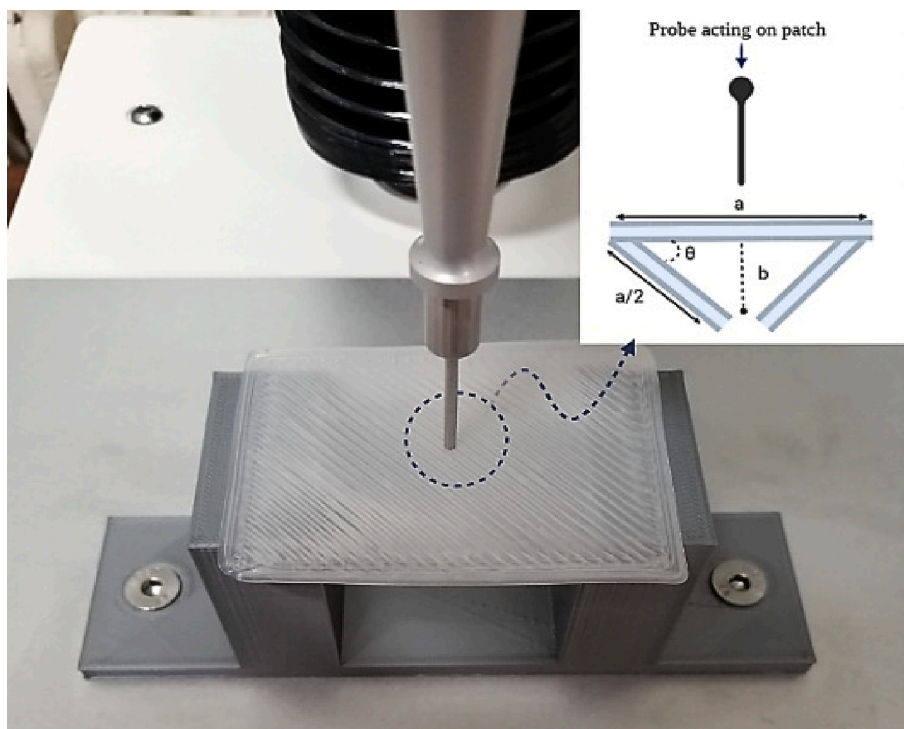


Fig. 1. Image of mechanical analysis of a 3D printed patch with texture analyzer; Box: illustration of the method used to measure the degree of flexibility of the 3D printed patches.

mobile phase was set at 1 mL/min, and a C18 (Agilent Poroshell 120, 150 × 4.6 mm, 5 μm) column (Agilent, USA) was used for analysis. The injection volume was set at 20 μL and the detection signal was recorded at 220 nm for ibuprofen and 274 nm for diclofenac sodium, keeping the analysis system at room temperature.

2.2.2.3. Mechanical properties. The break strength and degree of flexibility of the drug-loaded and blank printed patches were explored using a texture analyzer (TA.XT plus Texture Analyzer, Stable Micro Systems, UK) (Donnelly et al., 2010; Azizoğlu and Özer, 2020). A customized 3D printed apparatus was realized as support for attaching samples and was mounted on the working stage of the texture analyzer, as shown in Fig. 1. For all measurements, the texture analyzer was set in compression mode and an aluminum probe (2.0 mm in thickness) was moved into the middle of the patch at a speed of 2 mm/s. Considering the maximum peak of the force-distance curve, we extrapolated the break strength of the 3DP patches. As regards the degree of flexibility of each sample, it was calculated as the angle (θ) of patch bending upon break (Box of Fig. 1). The tangent of the angle was calculated using equation (1), and the bending angle was calculated with the arctangent formula (Equation (1)).

$$\tan\theta = \frac{b}{a/2} \quad (1)$$

where a is the initial length of the patch, b is the distance traveled by the probe before the patch was broken and θ is the angle determined at the point when the patch was broken.

2.2.2.4. Thermal analysis. The thermal behavior of pure starting materials (ibuprofen, diclofenac sodium, EVA 4030AC, and EVA 1821A) and printed formulations was investigated through differential scanning calorimetry (DSC 6000, Perkin Elmer, USA) and thermogravimetric analysis (TGA 4000, Perkin Elmer, USA). For TGA analysis, samples were equilibrated at 30 °C and heated up to 550 °C at a heating rate of 10 °C/min under a nitrogen flow rate of 30 mL/min, while recording the

weight loss. DSC measurements were carried out by placing the samples (around 5 mg) in aluminum pans. Samples were heated up with a heating rate of 10 °C/min from 30 °C to 180 °C, held for 3 min, then cooled down to -30 °C at 50 °C/min, held for 3 min, and lastly, heated up again to 180 °C at 10 °C/min. Diclofenac sodium samples were analyzed with the same method heating them up to 300 °C. Pyris Manager software (Perkin Elmer, USA) was used for data collection and analysis.

2.2.2.5. ATR-FTIR analysis. The structure analysis of raw materials and printed patches was conducted using attenuated total reflectance Fourier transformed infrared spectroscopy (ATR-FTIR, Spectrum Two FT-IR spectrometer with ATR accessory, Perkin Elmer, MA, USA). The samples were scanned 64 times with the spectra resolution of 4 cm⁻¹ at room temperature to obtain the ATR-FTIR spectra in a range of wave numbers from 4000 to 450 cm⁻¹.

2.2.3. In vitro drug release studies

The release profile of the printed patches was evaluated in a 50 % (v/v) ethanolic phosphate buffer saline (PBS at pH = 7.4) solution. All patches were weighed and then immersed in sealed glass bottles containing 100 mL of release medium. The bottles were incubated at 37 °C under stirring (100 rpm) for 48 h. At designated time points (1 h, 2 h, 4 h, 6 h, 24 h, and 48 h), 1 mL of release medium was taken out and replaced with an equal volume of the fresh one. The amount of ibuprofen and diclofenac sodium released from the patches was measured with HPLC as reported above. Triplicate measurements were made for each sample.

2.2.4. In vitro permeation studies

In vitro drug permeation studies were carried out using vertical diffusion cells (Franz cells) with a receptor compartment volume of 7 mL and an effective diffusion area of 1.766 cm². PBS (pH = 7.4) was used as receptor media and the receptor compartment was stirred continuously at 400 rpm by a magnetic stirrer. The system was thermostated at 32 ± 0.5 °C with a circulating jacket. The 3D-printed patches were mounted

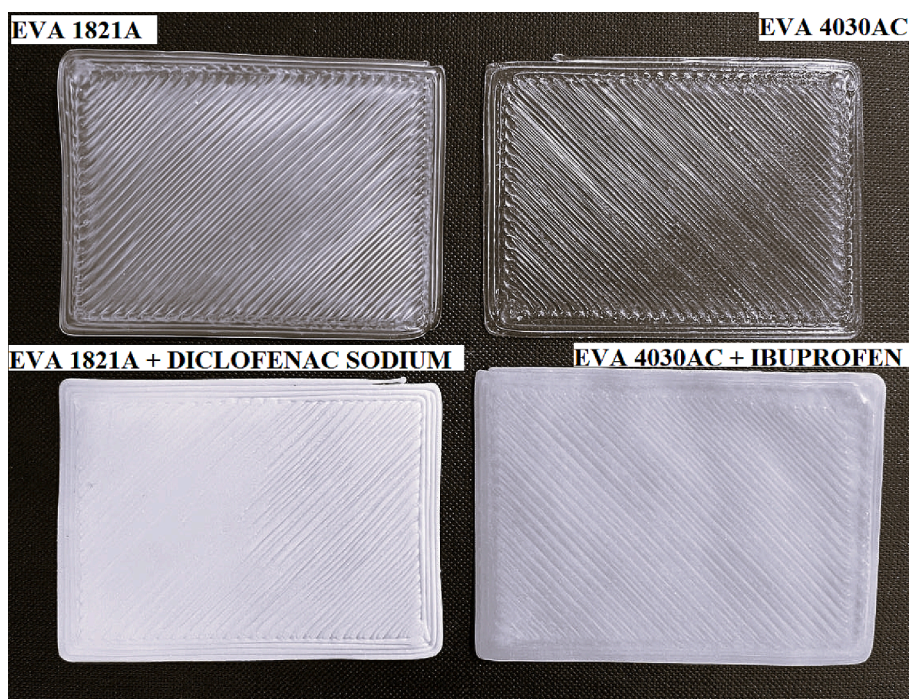


Fig. 2. Top view of drug-loaded and blank EVA-based transdermal patches.

Table 2

Analysis of weight and thickness of produced patches.

Sample (patch)	Average weight (g)	Average thickness (mm)
EVA 4030AC	2.52 ± 0.13	0.80 ± 0.01
EVA 1821A	2.80 ± 0.11	1.10 ± 0.01
EVA 4030AC + Ibuprofen	3.62 ± 0.02	1.01 ± 0.01
EVA 1821A + Diclofenac sodium	3.25 ± 0.01	1.02 ± 0.02

between the donor and receptor compartments, separated from the receptor by a Strat-M® membrane. Strat-M® is a commercially available skin-mimic artificial membrane that comprises a tight top layer coated

with a lipid blend and supported by two layers of polyethersulfone on top of one layer of polyolefin. This multi-layered structure allows the Strat-M® to simulate the morphology and the lipid chemistry of human skin (Haq et al., 2018). At defined sampling intervals (1 h, 2 h, 4 h, 6 h, 24 h, and 48 h), 0.2 mL of the receptor solution was withdrawn and replaced with an equal volume of fresh buffer. The amount of ibuprofen and diclofenac in all samples was then determined with HPLC as reported above. Triplicate measurements were made for each sample.

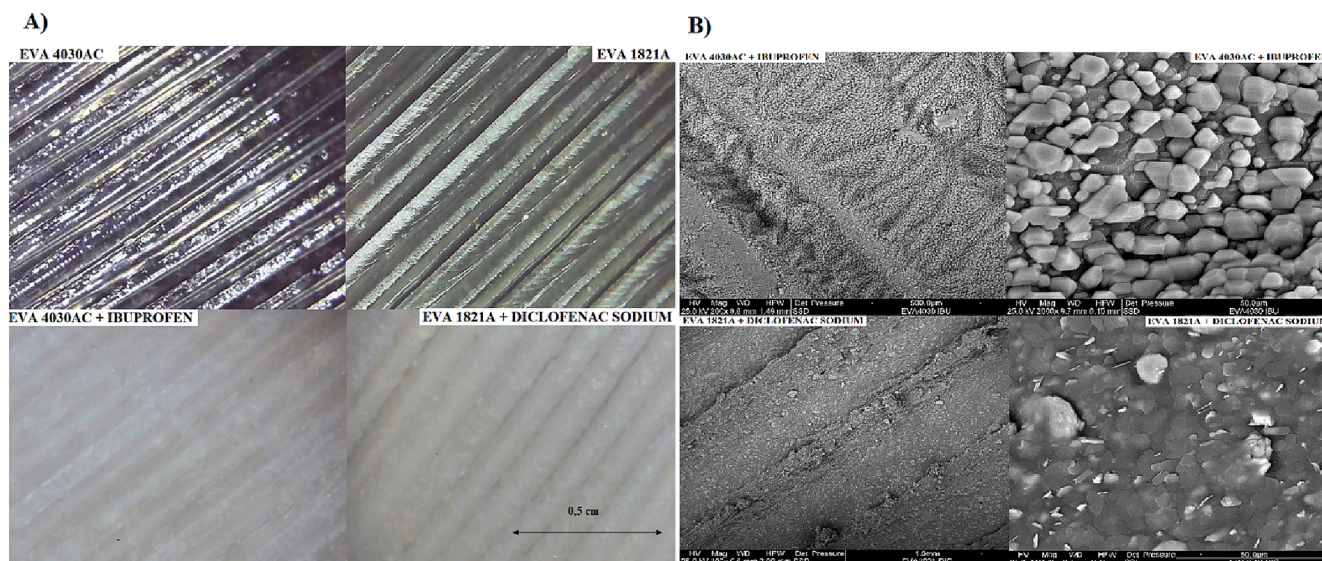


Fig. 3. A) ESEM images of drug-loaded and blank EVA patches; B) ESEM images showing the top view (left) and the close-up of the top view (right) of drug-loaded EVA patches.

3. Results and discussion

3.1. Characterization of 3D printed patches

3.1.1. Morphology and physicochemical properties

DPE technique was successfully employed for the first time to produce EVA-based transdermal patches (Fig. 2). EVA 4030AC and EVA 1821A were selected as polymeric matrices, thanks to their different physicochemical properties influenced by the percentage of vinyl acetate contained (40 % of VA and 18 % of VA respectively). Ibuprofen and diclofenac sodium were chosen as model drugs to demonstrate the adaptability of different EVA grades to drugs with significantly different thermal behavior to guarantee the printability of the desired patch. For this purpose, ibuprofen, which has melting and degradation temperatures much lower than those of diclofenac sodium, was printed in association with EVA 4030AC, which has a lower melting temperature than EVA 1821A. For the same reason, diclofenac sodium was printed in association with EVA 1821A.

The resulting patches were weighed immediately after the printing and their thickness was measured at six different points using a digital caliper. All the printed patches of each batch did not show significant differences in weight and thickness as reported in Table 2, suggesting that the reproducibility of the printing process was achieved.

The drug-loaded patches presented a whitish appearance compared with the transparent blank ones, due to the presence of the drug. EVA4030AC-based patches exhibited greater softness and transparency than those based on EVA 1821A according to the higher percentage of VA contained (Celanese, 2015b).

ESEM images confirmed the good printability of the mixtures as the individual layers of the patches appeared symmetrical (Fig. 3A). No porosity was detected by ESEM on the printed systems which probably came up with a slowing of the drug release rate. Diclofenac sodium was well-mixed with the polymer and uniformly distributed in the patch as no drug agglomerates were observed within the printed formulation. On the contrary, ibuprofen had partially deposited on the surface of the patch (Fig. 3B).

3.1.2. Content uniformity

The homogeneous distribution and the effective amount of ibuprofen and diclofenac sodium present in the samples were evaluated by cutting, weighing, and placing in ethanol different pieces of the drug-loaded patches. An HPLC measured the amount of drug dissolved in ethanol after 24 h. EVA 4030AC-based patches contained 74.6 ± 0.9 mg/g of ibuprofen proving an effective drug loading of 22.4 %. EVA 1821A-based patches contained 23.3 ± 0.7 mg/g of diclofenac sodium proving an effective drug loading of 7 %. Therefore, considering the average weight of drug-loaded printed patches (Table 2) the effective amount of ibuprofen and diclofenac was respectively 811 mg and 228 mg for one patch (Tiboni et al., 2021). The effective amount of diclofenac sodium loaded was much lower than that of ibuprofen. This can probably be explained by the better flowability of the mixture of ibuprofen and EVA 4030AC compared to the one of diclofenac sodium and EVA 1821A during the printing process. However, the printed patches proved to have a homogeneous distribution of the drug within them, given that the percentage of the drug dissolved in ethanol from the six portions of each patch after 24 h was comparable and with low standard deviation values (74.6 ± 0.9 % for the ibuprofen patch and 23.3 ± 0.7 % for the diclofenac sodium patch).

3.1.3. Break strength and degree of flexibility

The mechanical properties of produced 3D printed patches were evaluated with a texture analyzer. Flexibility tests were conducted on both drug-loaded and blank patches to ensure that these do not break during transport and use. The degree of flexibility was considered as the angle (θ) of patch bending upon break, while the value of break strength was extrapolated from the maximum peak of the force-distance curve.

Table 3

Maximum bending angles and break strengths of 3D printed patches.

Sample (patch)	Break strength (N)	Degree of flexibility (θ) ($^\circ$)
EVA 4030AC	5.7 ± 0.1	67.3 ± 0.5
EVA 1821A	31.7 ± 0.2	67.1 ± 0.5
EVA 4030AC + Ibuprofen	8.3 ± 0.1	61.2 ± 0.2
EVA 1821A + Diclofenac sodium	24 ± 0.1	67.5 ± 0.3

Table 4

Main parameters obtained from the thermal analysis of the samples.

Sample	T_{m1} ($^\circ$ C)	T_{m2} ($^\circ$ C)	T_{m3} ($^\circ$ C)	χ (%)	T_{onset} ($^\circ$ C)	T_d ($^\circ$ C)
EVA 4030AC powder	48	–	–	2	417	471
EVA 1821A powder	52	86	–	10	426	473
EVA 4030AC printed	42	–	–	2	–	–
EVA 1821A printed	44	86	–	14	–	–
EVA 4030AC + Ibuprofen	67	–	–	–	418	471
EVA 1821A + Diclofenac sodium	42	87	272	–	439	482
Ibuprofen	78	–	–	–	176	236
Diclofenac sodium	284	–	–	–	282	311

These calculated parameters are reported in Table 3. All samples showed a good degree of flexibility since they could bend to more than 60° , and the addition of ibuprofen and diclofenac sodium did not significantly affect the flexibility of the samples (Azizoglu et al., 2020). Moreover, EVA 4030AC-based patches were broken after applying less strength than was needed to break EVA 1821A-based patches due to the lower hardness of the polymer (Celanese, 2015a).

3.1.4. Thermal behavior

Thermal analyses were performed on pure materials to assess their melting and degradation temperatures and choose the most appropriate EVA grade for each model drug. As well the effect of drugs on the thermal behavior of EVAs after the printing process was investigated. The thermograms of pure materials and printed formulations are shown in Fig. 4, and their melting temperatures are reported in Table 4. Considering the thermograms of model drugs, ibuprofen melted at 78° C while diclofenac at 284° C. The endothermic peak at about 56° C of diclofenac sodium is probably due to the water evaporation from the surface of the drug (Arany et al., 2020) (Fig. 4B) since this peak disappears in the second heating scan (Supplementary Fig. DSC-S1b).

The thermogram of EVA 1821A powder showed two melting peaks ($T_{m1} = 52^\circ$ C and $T_{m2} = 86^\circ$ C), related to the presence of two types of crystals (polymorphs) in the structure of this polymer grade (Almeida et al., 2011; Genina et al., 2016). In the printed EVA1821A, the first peak fell at a lower temperature of 44° C; while the second peak changed to a broad shoulder with the T_m at 71° C, followed by the peak at 86° C (Fig. 4B). Since the thicker the crystal, the higher the melting temperature (Stark and Jaunich, 2011), both the melting temperature depression, as well as the presence of the new shoulder, could be attributed to the distribution of crystals with reduced thickness, because of the thermal treatment followed by rapid cooling during printing. This hypothesis is supported by the disappearance of the lower temperature peak and the shoulder in the second heating scan carried out after a controlled cooling (Supplementary Fig. DSC-S1b). Indeed, the controlled cooling allowed the polymer to crystallize into thicker crystals, typical of the starting powder.

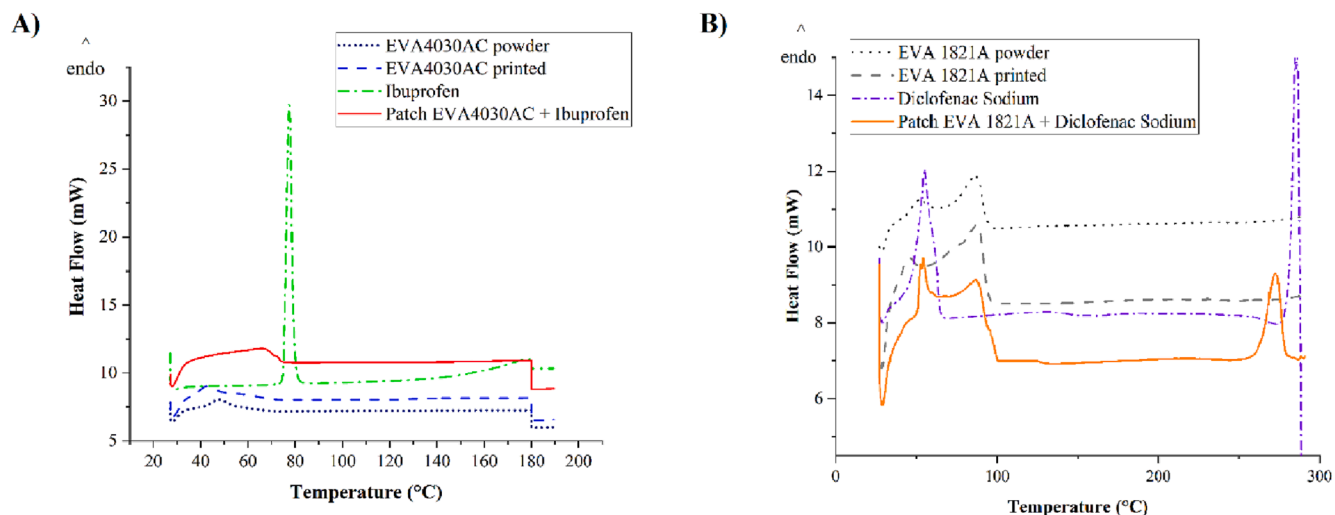


Fig. 4. DSC thermograms of the pure materials and 3D printed formulations.

EVA 4030AC powder had a net melting peak at 48 °C which shifted at a lower temperature of 42 °C in the printed polymer (Fig. 4A). Even in this case, the lowering of the melting peak could be attributed to the

presence of smaller crystals formed during rapid cooling. Indeed, the second heating scan carried out after the controlled cooling of the polymer showed only one melting peak at 48 °C related to crystals

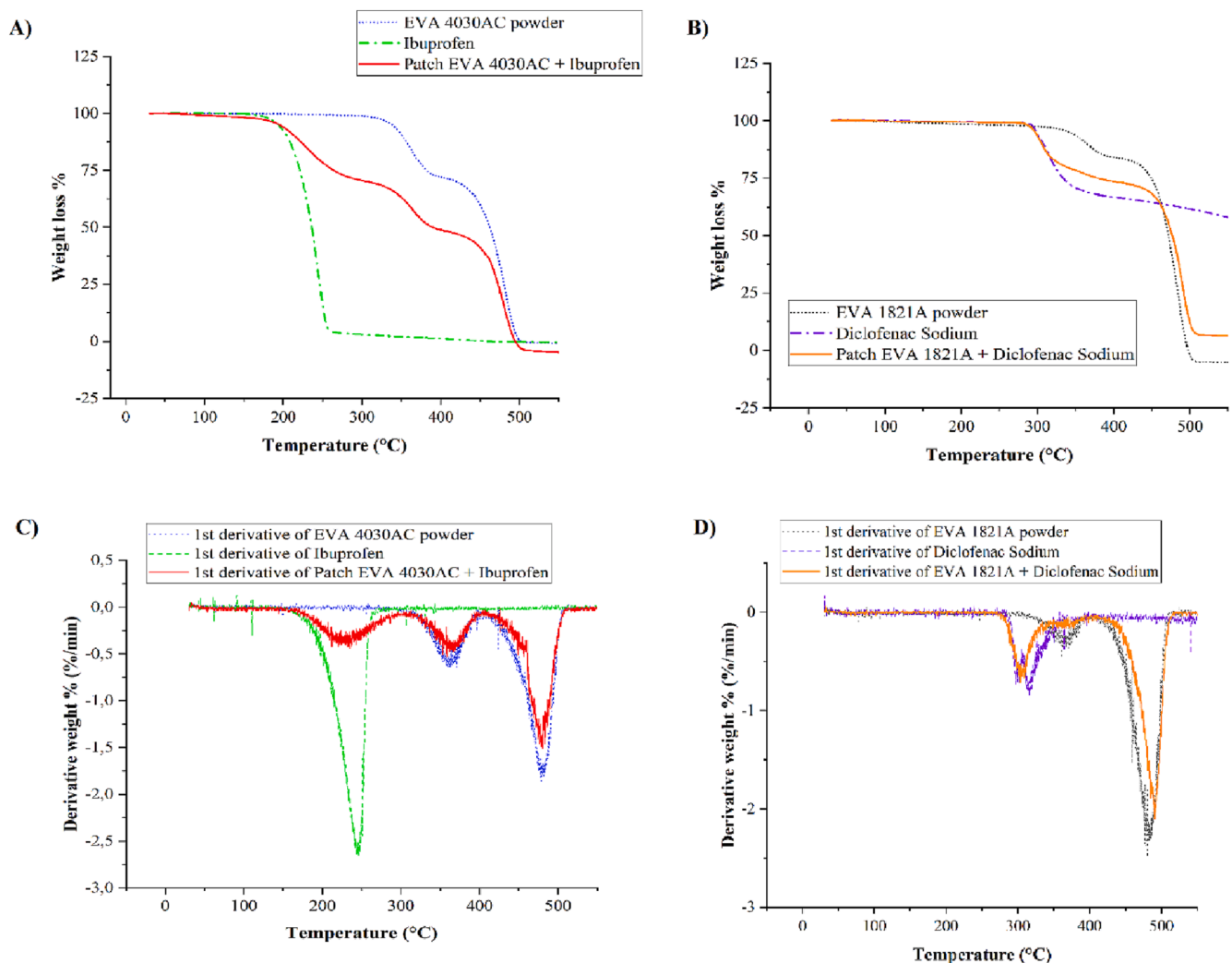


Fig. 5. A) TGA and C) DTG of pure ibuprofen, pure EVA 4030AC and EVA 4030AC/ibuprofen printed patch; B) TGA and D) DTG of pure diclofenac sodium, pure EVA 1821A and EVA 1821A/diclofenac sodium printed patch.

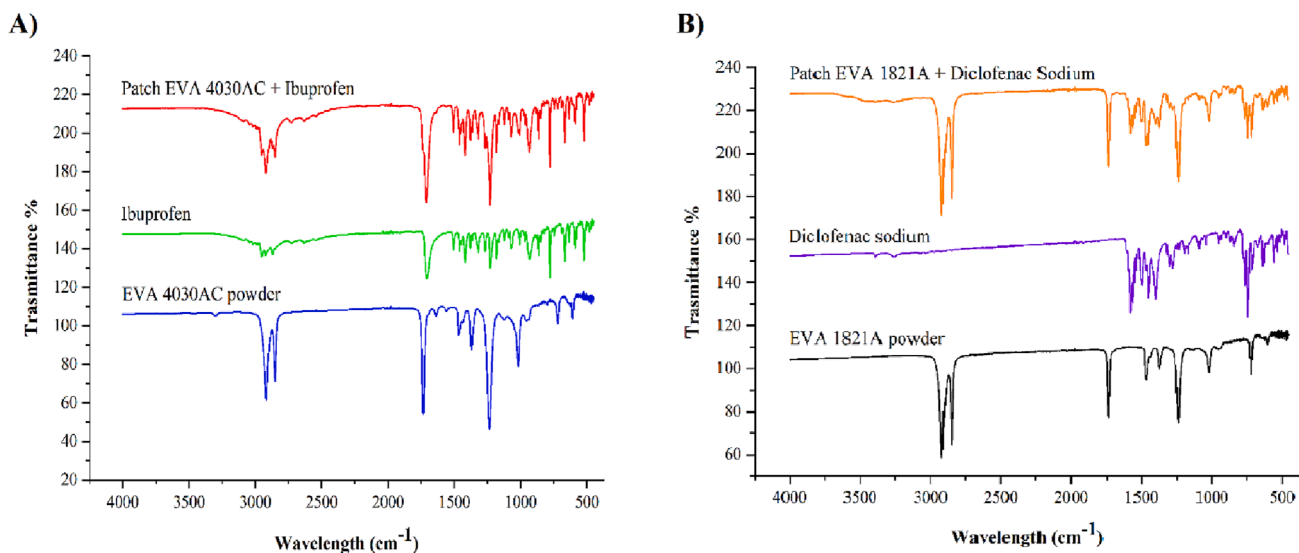


Fig. 6. Comparison of FTIR spectra of A) pure Ibuprofen, pure EVA 4030AC, and EVA 4030AC/Ibuprofen printed patch and B) pure Diclofenac sodium, pure EVA 1821A, and EVA 1821A/Diclofenac sodium printed patch.

typical of the starting powder (Supplementary Fig. DSC-S1a).

Since DSC analyses highlighted that EVA 1821A is a high-melting polymer while EVA 4030AC is a low-melting polymer, they were printed in association with diclofenac sodium and ibuprofen respectively, to avoid the alteration of the drug during the extrusion and low morphological quality of the printed products.

The DSC trace of the EVA 1821A with diclofenac showed the same endothermic peak of the printed EVA, suggesting that the drug did not modify the crystalline structure of the polymer (Fig. 4B). Diclofenac sodium melting peak shifted to a lower temperature (T_m at 272 °C) after printing and the drug was mostly in the crystalline form considering the melting enthalpy (ΔH_f) of diclofenac sodium powder (52.8 J/g) and printed (26.7 J/g). Despite the higher melting point of diclofenac sodium a limited amount of it melted during printing at 180 °C, probably as a result of the friction heat generated during processing, and did not recrystallize after cooling (Almeida et al., 2011).

Compared to the printed EVA, the patch of EVA4030AC loaded with ibuprofen showed a broad peak shifted to a higher temperature of 67 °C followed by a shoulder at 72 °C (Fig. 4A). There is no significant difference in the T_m of the EVA 4030AC melting peaks in the drug-free and drug-loaded patches. Therefore, the widening of this melting peak and the shift to higher temperatures could be due to a merge between the EVA melting peak and the ibuprofen melting peak, which shifted to a lower temperature after printing.

The depression of the melting point of both model drugs after printing could be attributed to the dissolution of the drug into the polymer matrix to some extent (Genina et al., 2016).

The samples' crystallinity degree (χ) was calculated according to equation (2) and tabulated in Table 4.

$$\chi(\%) = \left[\frac{\Delta H_f}{(\Delta H_f^* \cdot \Delta EVA)} \right] * 100 \quad (2)$$

where ΔH_f is the melting enthalpy of the analyzed EVA samples, ΔH_f^* is the tabulated melting enthalpy of the perfect polyethylene (PE) crystal ($\Delta H_f^* = 277.1 \text{ J/g}$), and ΔEVA is the weight fraction of EVA in the sample (Shi et al., 2008).

The degree of crystallinity of analyzed EVA powders and printed EVAs decreased as the VA content increased, since the VA-comonomer reduced the stereoregularity in the polymer chains, generating a decrease in the crystallinity of the PE segments (Wang and Deng, 2019). The higher crystallinity of printed EVA 1821A compared to the powder

could be attributed to the formation of crystals with reduced thickness causing a melting peak broadening. Therefore, the calculated crystallinity degree refers to all crystalline forms characterizing the printed polymer. Finally, in the drug loaded patches, particularly in the one loaded with ibuprofen, it was difficult to establish the degree of crystallinity of the EVA polymer since the melting peak of the drug, shifted to a lower temperature after printing, merged with that of the polymer.

Concerning the thermal stability of the samples, TGA analyses (Fig. 5A, B) were carried out to ensure the safe use of the selected drugs for 3D printing. The onset temperatures (T_{onset}) and the temperatures related to the maximum degradation rate (T_d) were calculated through DTG (Fig. 5C, D) and are presented in Table 4. Both model drugs proved to stay stable at processing temperature with a weight loss of approximately 2 % at 176 °C for ibuprofen and 283 °C for diclofenac sodium. Pure EVAs presented two weight losses: a small degradation phase at a lower temperature (T_{onset} of 319 °C with a T_d of 352 °C for EVA 4030AC and T_{onset} of 328 °C with a T_d of 364 °C for EVA 1821A) which is due to acetic acid loss and the main degradation phase at a higher temperature (T_{onset} of 417 °C with a T_d of 471 °C for EVA 4030AC and T_{onset} of 426 °C with a T_d of 473 °C for EVA 1821A) which is due to fragments of the polymer backbone (Díez et al., 2021). EVA-based loaded patches degraded with the same trend as pure EVAs and at approximately the same temperatures, demonstrating that drugs did not reduce the thermal stability of the polymers.

3.1.5. Investigation of chemical characteristics through ATR-FTIR spectroscopy

ATR-FTIR analyses were conducted to obtain further information on the chemical composition of 3D printed patches and to investigate whether interactions between the polymer and drug had occurred. FTIR spectra of pure materials and 3D printed formulations are compared in Fig. 6.

As it can be observed, both spectra of 3D printed patches presented the characteristic peak of EVA polymer at 1737 cm^{-1} related to a carbonyl C=O stretching (Genina et al., 2016). The spectrum of the printed EVA 4030AC/Ibuprofen patch showed the absorption band of C=O and OH functional groups of ibuprofen at 1714 cm^{-1} and 2995 cm^{-1} respectively (Elkordy and Ebtessam, 2010). The spectrum of the printed EVA 1821A/Diclofenac sodium patch showed the absorption band of C=C, OH, and NH functional groups of diclofenac sodium at 1575 cm^{-1} , 3260 cm^{-1} , and 3387 cm^{-1} respectively (Swain et al., 2015). This suggested that both the polymer and drug were effectively

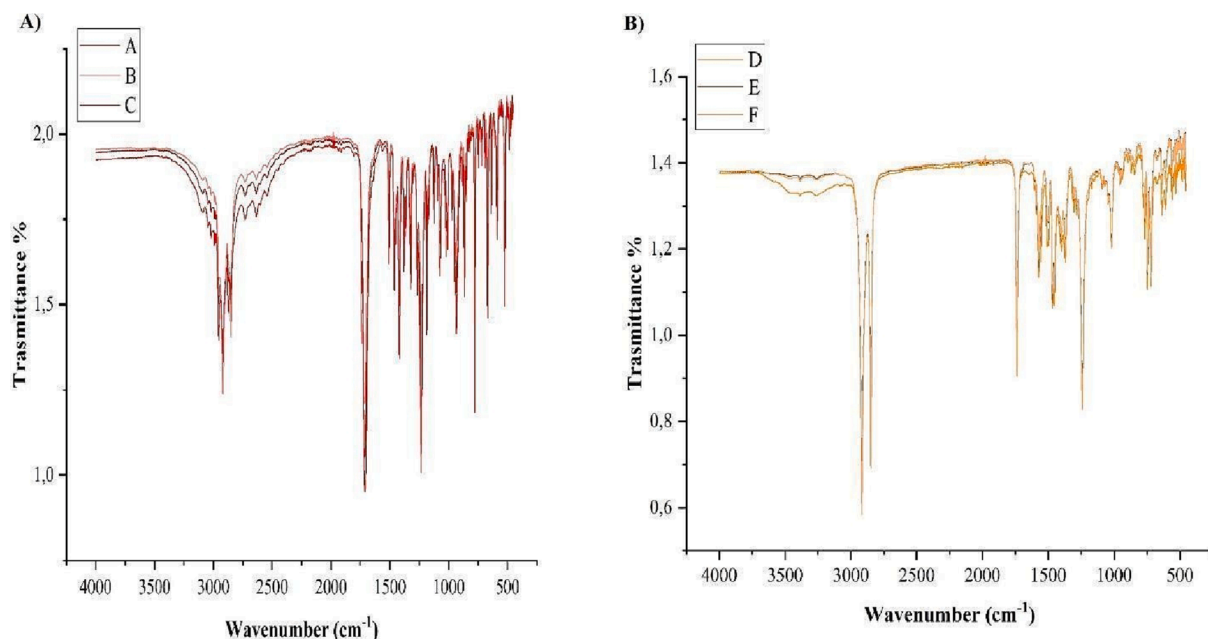


Fig. 7. Composition homogeneity of A) EVA 4030AC/Ibuprofen printed patches and B) EVA 1821A/Diclofenac sodium printed patches.

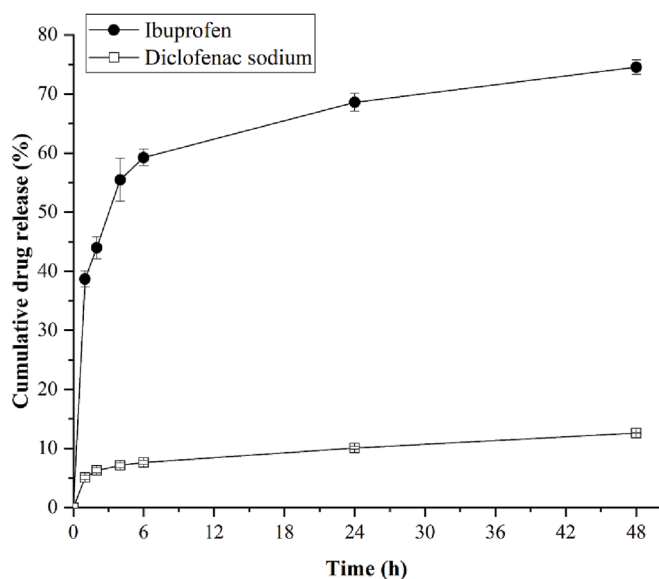


Fig. 8. In vitro release profiles of Ibuprofen and Diclofenac sodium from EVA 4030AC and EVA 1821A-based patches respectively. All values are presented as mean \pm SD, where $n = 3$.

incorporated into the final formulations. No new chemical bonds were established for EVA during the printing process since the spectra of the pure materials and final formulations were found to be similar. Moreover, the homogeneous distribution of the drug within the printed devices was evaluated by analyzing random portions of the samples with FTIR. The resulting spectra were normalized with the EVA absorption at 1737 cm^{-1} as a reference and reported in Fig. 7 (Moroni et al., 2022). In agreement with content uniformity analysis, the printed patches proved to have a homogeneous composition considering that no notable differences in the intensities of the characteristic peaks of the drugs were found.

3.2. In vitro ibuprofen and diclofenac sodium release and permeation profiles

Drug release from 3D printed patches was tested in a mixture of 50 % ethanol in PBS (pH = 7.4) considering the poor solubility of the model drugs in water (Friuli et al., 2018). Fig. 8 illustrates the cumulative percentage of ibuprofen and diclofenac sodium released from EVA patches over a period of 48 h.

Both formulations exhibited an initial burst release phase in the first 6 h followed by a steady release phase. The initial fast release might be contributed by the instantaneous dissolution of surface-bound drug molecules in the release medium (Tang et al., 2010), while the subsequent slowing of the release rate is probably attributed to the diffusion of drug molecules through the polymer matrix. Diclofenac sodium showed a minimal “burst” effect which could be attributed to its more homogeneous distribution in the polymer matrix, while a remarkable amount of ibuprofen stayed on the surface of the matrix and was easily released (Fig. 3B). Despite the presence of ethanol in the dissolution medium, the release rate of model drugs from the patches was overall slow, probably due to the hydrophobic and non-swelling nature of EVA polymer. In addition, the lack of a porous structure (Fig. 3B) contributed to limit the fluid uptake of EVA matrices, slowing down the drugs’ diffusion through them and dissolution into the release medium. Consequently, a fraction of the drugs remained entrapped by the EVA’s hydrophobic chains (Almeida et al., 2012). The cumulative release of ibuprofen was 366.65 mg and that of diclofenac sodium was 49.26 mg after 48 h (74.5 % and 12.6 % of the total amount present in one patch respectively). These results are consistent with previous studies (Tallury et al., 2007; Shin and Lee, 2002) which demonstrated that the vinyl acetate content of EVA copolymer affected the drug release rate. An increase in permeability of the polymer and a consequent increase in the release rate was observed with an increment in VA content, as the introduction of amorphous VA comonomer to a highly crystalline polyethylene decreases the crystallinity of the system and improves the microporosity of the whole matrix (Kamath and Wakefield, 1965). Effectively, DSC analyses confirmed that EVA 1821A possesses a higher crystalline structure than EVA 4030AC. In this way, by varying the grade of EVA copolymer the drug’s permeation rate through EVA membranes can be tailored, representing an important advantage for personalized transdermal therapies. Although the release rate from EVA matrices is

Table 5
Kinetics parameters of drug release studies.

Drug	Korsmeyer-Peppas			Peppas-Sahlin		
	k	N	R ²	K _d (h ^{-0.45})	K _r (h ^{-0.45})	R ²
Ibuprofen	42 ± 2	0.15 ± 0.02	0.987	36 ± 2	-4.1 ± 0.5	0.954
Diclofenac Sodium	5.2 ± 0.1	0.22 ± 0.01	0.995	4.5 ± 0.4	-0.42 ± 0.08	0.944

often a strong function of the VA content in the polymer, it could be also dependent on the drug loading to some extent. The higher drug loading allowed ibuprofen to better diffuse through the matrix, as the porous network path, created by drug crystals in a non-porous system and connected with the surface, allowed the drug to be released (Almeida et al., 2011).

Furthermore, to clarify the kinetics of ibuprofen and diclofenac sodium release from EVA patches the data obtained from release profiles were fitted by Korsmeyer-Peppas (equation (3)) and Peppas-Sahlin (equation (4)) models.

$$\frac{M_t}{M_\infty} = kt^n \quad (3)$$

$$\frac{M_t}{M_\infty} = K_d t^m + K_r t^{2m} \quad (4)$$

where $\frac{M_t}{M_\infty}$ is a fraction of drug released at time t, k is the release rate constant, n is the release exponent, K_d is the diffusion constant, K_r is the relaxation constant, and m is the Fickian diffusion exponent (Mehran et al., 2020).

The correlation coefficients (R²) and constants of each model are shown in Table 5, and the release data fitting to each model are shown in Fig. 9. Considering the correlation coefficient (R²) both models well described the release kinetics of ibuprofen (0.987, 0.954) and diclofenac sodium (0.995, 0.944). In the Korsmeyer-Peppas model, the n values less than 0.5 reflected a quasi-Fickian diffusion mechanism which indicates the drug release through non-swallowable matrix diffusion (Paarakh et al., 2018). Moreover, to determine the predominant mechanism among drug diffusion and polymer relaxation, the drug release profile of all formulations was fitted to the Peppas-Sahlin equation. The higher value of K_d than K_r indicates that Fickian diffusion was the predominant mechanism of drug release from the matrices than polymer relaxation and swelling in such matrix (Baggi and Kilaru, 2016).

Additionally, the *in vitro* ibuprofen and diclofenac sodium

permeation behavior was determined using vertical diffusion cells. An artificial Strat-M® membrane was selected as the partitioning membrane since it was reported to have comparable results to human skin (Haq et al., 2018). The *in vitro* permeation profiles represented in Fig. 10 indicate that ibuprofen reached a higher permeation (642.1 µg/cm²) compared to the diclofenac sodium (394.22 µg/cm²) over the 48 h of experimentation. These results are consistent with that of release studies where it was found that the EVA 4030AC-based patch possessed a faster release behavior than the one based on EVA 1821A. Despite this, the difference in trends between the release and permeation profiles of each model drug is probably attributed to the complex composition of the partition membrane used in drug permeation studies. In fact, Strat-M® membrane mimics the percutaneous absorption of the drug, a process that involves steps such as the drug's release and dissolution from the formulation, its partition and diffusion across the stratum corneum, and its penetration into the skin's layers. Consequently, permeation through Strat-M® membrane is influenced by many factors, including not only the characteristics of the drug delivery system but also the

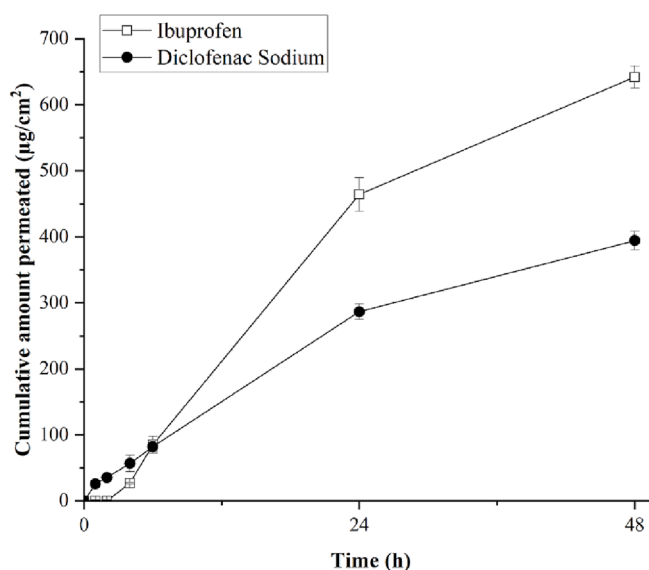


Fig. 10. *In vitro* permeation profiles of Ibuprofen and Diclofenac sodium through Strat-M® membrane from EVA 4030AC and EVA 1821A-based patches respectively. All values are presented as mean ± SD, where n = 3.

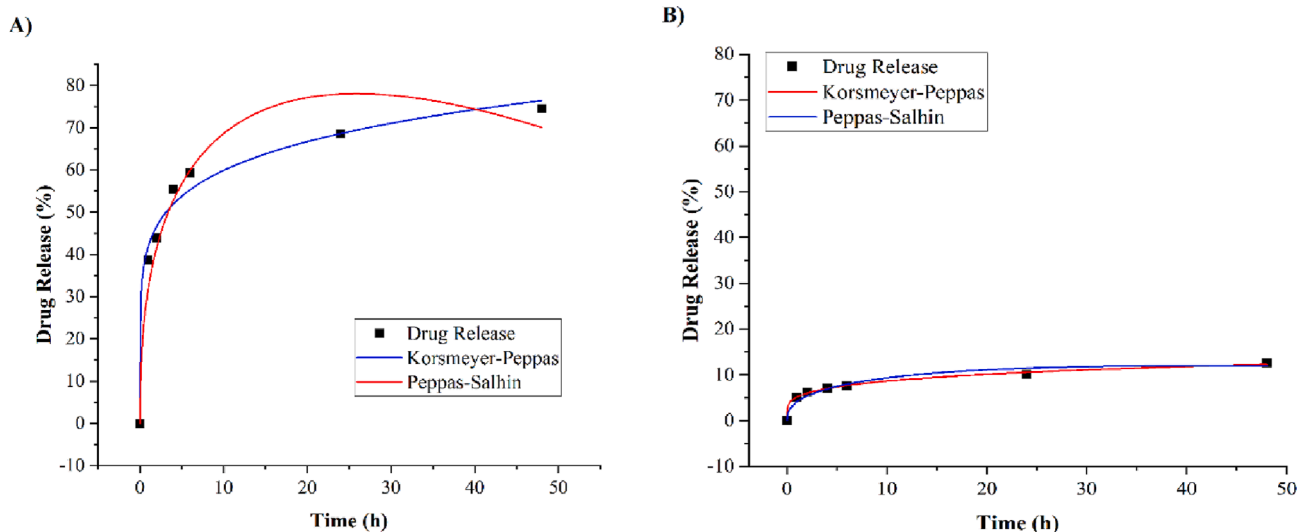


Fig. 9. Release data of A) Ibuprofen and B) Diclofenac sodium fitting to Korsmeyer-Peppas and Peppas-Sahlin models.

physicochemical properties of the drug, e.g. lipophilicity, solubility, molecular weight, and pKa (Bolla et al., 2020). Indeed, previous findings (Pradal, 2020) revealed that ibuprofen permeates through human skin to a greater extent than diclofenac sodium due to its lower molecular weight and higher pKa value which could affect the drug permeation rate.

4. Conclusions

This work demonstrated, for the first time, the application of EVA and 3DP-DPE as potential tools for manufacturing transdermal patches that can be customized according to the patient's needs, thanks to the polymer's tailorable properties and compatibility with different drugs. Both chosen formulations showed excellent processability via the DPE technique, ensuring the thermal stability of the active compounds and good morphological quality of the extrudates. 3D-printed transdermal patches also exhibited adequate flexibility which prevents breakage during transport and use. Moreover, the VA content of the polymer seemed to affect the polymer crystallinity and the permeability of the extruded EVA matrix. Consequently, by selecting the appropriate EVA grade, the drug release behavior of EVA patches could be influenced, considering that it could also depend on other factors, including drug crystallinity and drug loading. Therefore, by coupling the versatile physicochemical and mechanical properties of EVA excipient and the ease of use of DPE technology, it is believed that the 3D-printed EVA-based transdermal patches can be scalable for a potential practical application in pharmacies and hospitals.

Funding

Sofia Moroni acknowledge Marche Region for the PhD scholarship (Innovative doctoral programme POR Marche FSE 2014/2020 D.R. 354/2020).

This research received funding from Regione Marche (Italy) POR MARCHE FESR 2014–2020 - Asse 1 – OS 2 – Azione 2.1 <https://www.marchebiobank.it>.

CRedit authorship contribution statement

Giorgia Maurizii: Methodology, Investigation, Formal analysis, Data curation, Writing – original draft. **Sofia Moroni:** Methodology, Investigation, Data curation. **Shiva Khorshid:** Investigation, Data curation. **Annalisa Aluigi:** Methodology, Data curation, Writing – review & editing. **Mattia Tiboni:** Conceptualization, Supervision, Methodology, Formal analysis, Data curation, Writing – review & editing. **Luca Casertari:** Conceptualization, Resources, Funding acquisition, Project administration, Supervision, Writing – review & editing.

Declaration of Competing Interest

The authors declare that they have no known competing financial interests or personal relationships that could have appeared to influence the work reported in this paper.

Data availability

Data will be made available on request.

Acknowledgements

We would like to express our sincere gratitude to Celanese for their contribution to this research and for providing Celanese EVA (ethylene vinyl acetate) used in this study as well as the support to article review. Moreover, we acknowledge ITIS E. Mattei (Urbino, PU, Italy) for the utilization of FT-IR instrument.

Appendix A. Supplementary material

Supplementary data to this article can be found online at <https://doi.org/10.1016/j.ijpharm.2023.122720>.

References

- Almeida, A., Possemiers, S., Boone, M.N., De Beer, T., Quinten, T., Van Hoorebeke, L., Remon, J.P., Vervaeck, C., 2011. Ethylene vinyl acetate as a matrix for oral sustained release dosage forms produced via hot-melt extrusion. *Eur. J. Pharm. Biopharm.* 77 (2), 297–305. <https://doi.org/10.1016/j.ejpb.2010.12.004>.
- Almeida, A., Brabant, L., Siepmann, F., De Beer, T., Bouquet, W., Van Hoorebeke, L., Siepmann, J., Remon, J.P., Vervaeck, C., 2012. Sustained release from hot-melt extruded matrices based on ethylene vinyl acetate and polyethylene oxide. *Eur. J. Pharm. Biopharm.* 82 (3), 526–533. <https://doi.org/10.1016/j.ejpb.2012.08.008>.
- Annaji, M., Ramesh, S., Poudel, L., Govindarajulu, M., Arnold, R.D., Dhanasekaran, M., Babu, R.J., 2020. Application of extrusion-based 3D printed dosage forms in the treatment of chronic diseases. *J. Pharm. Sci.* 109 (12), 3551–3568. <https://doi.org/10.1016/j.xphs.2020.09.042>.
- Arany, P., Papp, I., Zichar, M., Csontos, M., Elek, J., Regdon, G., Budai, I., Béres, M., Gesztelyi, R., Fehér, P., Ujhelyi, Z., Vasvári, G., Haimhoffer, Á., Fenyvesi, F., Váradi, J., Miklós, V., Bácskay, I., 2020. In vitro tests of FDM 3D-printed diclofenac sodium-containing implants. *Molecules* 25 (24), 5889. <https://doi.org/10.3390/molecules25245889>.
- Azizoğlu, E., Özer, Ö., 2020. Fabrication of montelukast sodium loaded filaments and 3D printing transdermal patches onto packaging material. *Int. J. Pharm.* 587, 119588. <https://doi.org/10.1016/j.ijpharm.2020.119588>.
- Baggi, R.B., Kilaru, N.B., 2016. Calculation of predominant drug release mechanism using Peppas-Sahlin model, part-I (substitution method): A linear regression approach. *Asian J. Pharmacy Technol.* 6 (4), 223. <https://doi.org/10.5958/2231-5713.2016.00033.7>.
- Bolla, P.K., Clark, B.A., Juluri, A., Cheruvu, H.S., Renukuntla, J., 2020. Evaluation of formulation parameters on permeation of ibuprofen from topical formulations using Strat-M® membrane. *Pharmaceutics* 12 (2), 151. <https://doi.org/10.3390/pharmaceutics12020151>.
- Boniatti, J., Januskaite, P., Fonseca, L.B., Viçosa, A.L., Amendoeira, F.C., Tuleu, C., Basit, A.W., Goyanes, A., Ré, M.-I., 2021. Direct powder extrusion 3D printing of praziquantel to overcome neglected disease formulation challenges in paediatric populations. *Pharmaceutics* 13 (8), 1114. <https://doi.org/10.3390/pharmaceutics13081114>.
- Borandeh, S., van Bochove, B., Teotia, A., Seppälä, J., 2021. Polymeric drug delivery systems by additive manufacturing. *Adv. Drug Deliv. Rev.* 173, 349–373. <https://doi.org/10.1016/j.addr.2021.03.022>.
- Celanese, 2015a. Potential use of ethylene vinyl acetate copolymer excipient in Oral Controlled Release Applications: A literature review. <https://explore.celanese.com/eva-in-oral-controlled-release-whitepaper-download> (accessed October 6, 2022).
- Celanese, 2015b. Injection molding guide for LDPE and Eva Copolymers. <https://automotive.celanese.com/-/media/EVA-Polymers/Files/Product-Technical-Guides/EVA-016-PlasticsMoldingGuide-TG-EN-1115.pdf> (accessed October 6, 2022).
- Díez, E., Rodríguez, A., Gómez, J.M., Galán, J., 2021. Tg and DSC as tools to analyse the thermal behaviour of Eva Copolymers. *J. Elastomers Plast.* 53 (7), 792–805. <https://doi.org/10.1177/0095244320988163>.
- Donnelly, R.F., Majithiya, R., Singh, T.R., Morrow, D.I., Garland, M.J., Demir, Y.K., Migalska, K., Ryan, E., Gillen, D., Scott, C.J., Woolfson, A.D., 2010. Design, optimization and characterisation of polymeric microneedle arrays prepared by a novel laser-based micromoulding technique. *Pharm. Res.* 28 (1), 41–57. <https://doi.org/10.1007/s11095-010-0169-8>.
- Elkordy, A.A., Ebtessam, A., 2010. Dissolution of Ibuprofen from spray dried and spray chilled particles. *Pak. J. Pharm. Sci.* 23 (3), 284–290.
- Fanous, M., Gold, S., Muller, S., Hirsch, S., Ogorcka, J., Imanidis, G., 2020. Simplification of fused deposition modeling 3D-Printing Paradigm: Feasibility of 1-step direct powder printing for immediate release dosage form production. *Int. J. Pharm.* 578, 119124. <https://doi.org/10.1016/j.ijpharm.2020.119124>.
- Friuli, V., Bruni, G., Musitelli, G., Conte, U., Maggi, L., 2018. Influence of dissolution media and presence of alcohol on the in vitro performance of pharmaceutical products containing an insoluble drug. *J. Pharm. Sci.* 107 (1), 507–511. <https://doi.org/10.1016/j.xphs.2017.06.001>.
- Genina, N., Holländer, J., Jukarainen, H., Mäkilä, E., Salonen, J., Sandler, N., 2016. Ethylene vinyl acetate (EVA) as a new drug carrier for 3D printed medical drug delivery devices. *Eur. J. Pharm. Sci.* 90, 53–63. <https://doi.org/10.1016/j.ejps.2015.11.005>.
- Goyanes, A., Allahham, N., Trenfield, S.J., Stoyanov, E., Gaisford, S., Basit, A.W., 2019. Direct powder extrusion 3D printing: Fabrication of drug products using a novel single-step process. *Int. J. Pharm.* 567, 118471. <https://doi.org/10.1016/j.ijpharm.2019.118471>.
- Haq, A., Goodyear, B., Ameen, D., Joshi, V., Michniak-Kohn, B., 2018. Strat-M® synthetic membrane: Permeability comparison to human cadaver skin. *Int. J. Pharm.* 547 (1–2), 432–437. <https://doi.org/10.1016/j.ijpharm.2018.06.012>.
- Kamath, P.M., Wakefield, R.W., 1965. Crystallinity of ethylene-vinyl acetate copolymers. *J. Appl. Polym. Sci.* 9 (9), 3153–3160. <https://doi.org/10.1002/app.1965.070090919>.
- Mehran, M., Masoum, S., Memarzadeh, M., 2020. Microencapsulation of Mentha spicata essential oil by spray drying: Optimization, characterization, release kinetics of

- essential oil from microcapsules in food models. *Ind. Crop. Prod.* 154, 112694 <https://doi.org/10.1016/j.indcrop.2020.112694>.
- Moroni, S., Khorshid, S., Aluigi, A., Tiboni, M., Casettari, L., 2022. Poly(3-hydroxybutyrate): A potential biodegradable excipient for direct 3D printing of Pharmaceuticals. *Int. J. Pharm.* 623, 121960 <https://doi.org/10.1016/j.ijpharm.2022.121960>.
- Ong, J.J., Awad, A., Martorana, A., Gaisford, S., Stoyanov, E., Basit, A.W., Goyanes, A., 2020. 3D printed opioid medicines with alcohol-resistant and abuse-deterrent properties. *Int. J. Pharm.* 579, 119169 <https://doi.org/10.1016/j.ijpharm.2020.119169>.
- Paarakh, M.P., Jose, P.A., Setty, C.M., Christoper, G.V.P., 2018. Release Kinetics-Concepts and Applications. *International Journal of Pharmacy Research & Technology* 8 (1), 12–20.
- Pistone, M., Racaniello, G.F., Arduino, I., Laquintana, V., Lopalco, A., Cutrignelli, A., Rizzi, R., Franco, M., Lopodota, A., Denora, N., 2022. Direct cyclodextrin-based powder extrusion 3D printing for one-step production of the BCS class II model drug niclosamide. *Drug Deliv. Transl. Res.* 12 (8), 1895–1910. <https://doi.org/10.1007/s13346-022-01124-7>.
- Pistone, M., Racaniello, G.F., Rizzi, R., Iacobazzi, R.M., Arduino, I., Lopalco, A., Lopodota, A.A., Denora, N., 2023. Direct cyclodextrin based powder extrusion 3D printing of Budesonide loaded mini-tablets for the treatment of eosinophilic colitis in paediatric patients. *Int. J. Pharm.* 632, 122592 <https://doi.org/10.1016/j.ijpharm.2023.122592>.
- Pradal, J., 2020. Comparison of skin permeation and putative anti-inflammatory activity of commercially available topical products containing ibuprofen and diclofenac. *J. Pain Res.* 13, 2805–2814. <https://doi.org/10.2147/jpr.s262390>.
- Durga Prasad Reddy, R., Sharma, V., 2020. Additive Manufacturing in Drug Delivery Applications: A Review. *Int. J. Pharm.* 589, 119820 <https://doi.org/10.1016/j.ijpharm.2020.119820>.
- Samaro, A., Shaqour, B., Goudarzi, N.M., Ghijs, M., Cardon, L., Boone, M.N., Verleije, B., Beyers, K., Vanhoorne, V., Cos, P., Vervaet, C., 2021. Can filaments, pellets and powder be used as feedstock to produce highly drug-loaded ethylene-vinyl acetate 3D printed tablets using extrusion-based additive manufacturing? *Int. J. Pharm.* 607, 120922 <https://doi.org/10.1016/j.ijpharm.2021.120922>.
- Sánchez-Guirales, S.A., Jurado, N., Kara, A., Lalatsa, A., Serrano, D.R., 2021. Understanding direct powder extrusion for fabrication of 3D printed personalised medicines: A case study for nifedipine minitables. *Pharmaceutics* 13 (10), 1583. <https://doi.org/10.3390/pharmaceutics13101583>.
- Schneider, C., Langer, R., Loveday, D., Hair, D., 2017. Applications of ethylene vinyl acetate copolymers (EVA) in Drug Delivery Systems. *J. Control. Release* 262, 284–295. <https://doi.org/10.1016/j.jconrel.2017.08.004>.
- Seoane-Viaño, I., Trenfield, S.J., Basit, A.W., Goyanes, A., 2021. Translating 3D printed pharmaceuticals: From hype to real-world clinical applications. *Adv. Drug Deliv. Rev.* 174, 553–575. <https://doi.org/10.1016/j.addr.2021.05.003>.
- Shi, X.M., Zhang, J., Jin, J., Chen, S.J., 2008. Non-isothermal crystallization and melting of ethylene-vinyl acetate copolymers with different vinyl acetate contents. *Express Polym Lett* 2 (9), 623–629. <https://doi.org/10.3144/expresspolymlett.2008.75>.
- Shin, S.C., Lee, H.-J., 2002. Controlled release of triprolidine using ethylene-vinyl acetate membrane and Matrix Systems. *Eur. J. Pharm. Biopharm.* 54 (2), 201–206. [https://doi.org/10.1016/s0939-6411\(02\)00051-6](https://doi.org/10.1016/s0939-6411(02)00051-6).
- Stark, W., Jaunich, M., 2011. Investigation of ethylene/vinyl acetate copolymer (EVA) by Thermal Analysis DSC and DMA. *Polym. Test.* 30 (2), 236–242. <https://doi.org/10.1016/j.polymertesting.2010.12.003>.
- Swain, R., Nagamani, R., Panda, S., 2015. Formulation, in vitro characterization and stability studies of fast dispersing tablets of diclofenac sodium. *J. Appl. Pharm. Sci.* 094–102 <https://doi.org/10.7324/japs.2015.50715>.
- Tallury, P., Alimohammadi, N., Kalachandra, S., 2007. Poly(ethylene-co-vinyl acetate) copolymer matrix for delivery of chlorhexidine and acyclovir drugs for use in the oral environment: Effect of drug combination, copolymer composition and coating on the drug release rate. *Dent. Mater.* 23 (4), 404–409. <https://doi.org/10.1016/j.dental.2006.02.011>.
- Tang, M., Hou, J., Lei, L., Liu, X., Guo, S., Wang, Z., Chen, K., 2010. Preparation, characterization and properties of partially hydrolyzed ethylene vinyl acetate copolymer films for Controlled Drug Release. *Int. J. Pharm.* 400 (1–2), 66–73. <https://doi.org/10.1016/j.ijpharm.2010.08.031>.
- Tiboni, M., Campana, R., Frangipani, E., Casettari, L., 2021. 3D printed clotrimazole intravaginal ring for the treatment of recurrent vaginal candidiasis. *Int. J. Pharm.* 596, 120290 <https://doi.org/10.1016/j.ijpharm.2021.120290>.
- Vaz, V.M., Kumar, L., 2021. 3D printing as a promising tool in personalized medicine. *AAPS PharmSciTech* 22 (1). <https://doi.org/10.1208/s12249-020-01905-8>.
- Wang, K., Deng, Q., 2019. The thermal and mechanical properties of poly(ethylene-co-vinyl acetate) random copolymers (PEVA) and its covalently crosslinked analogues (cpeva). *Polymers* 11 (6), 1055. <https://doi.org/10.3390/polym11061055>.
- Xu, P., Li, J., Meda, A., Osei-Yeboah, F., Peterson, M.L., Repka, M., Zhan, X., 2020. Development of a quantitative method to evaluate the printability of filaments for fused deposition modeling 3D printing. *Int. J. Pharm.* 588, 119760 <https://doi.org/10.1016/j.ijpharm.2020.119760>.